Optimizations electrophoretic deposition of PEEK/HA on 316L for biomedical application

Hayder Hashim Mohammed
Dept. production Engineering and metallurgy, University of Technology, Baghdad, Iraq.

Makarim Hazim Abdlkareem
Dept. production Engineering and metallurgy, University of Technology, Baghdad, Iraq.

Ali Mundher Mustafa
Dept. production Engineering and metallurgy, University of Technology, Baghdad, Iraq.

ABSTRACT

In this study, two types of current were used (DC and AC current), to deposit (PEEK/HA system) on 316L by EPD. Taguchi approach with L9 array was carried out in order to obtain the best deposition conditions for (Polyethetherketone/Hydroxyapatite) coating layer. The parameters that used for deposition are (concentration, degree of grinding, time and voltage). The stability of the solutions was determined using zeta potential tests. Scanning electron microscopy and X-ray diffraction were used to evaluate the deposited coating microstructurally. Coating layers were characterized for thickness, porosity and atomic force microscopy (AFM). The Taguchi design of trials indicated that the optimal conditions for PEEK/HA DC depositing are (90 Voltage ,3 minutes, and 4% C, 0.06 m, which equated to 500 emery paper SiC). The optimum PEEK/HA DC and PEEK/HA AC coating was evaluated based on adhesion of coating with substrate. The results showed that the optimum sample with DC current deposition had better adhesion with a removal area of (9%) as compared to (11%) for the AC optimum sample. The corresponding thickness, porosity and nanoroughness for optimum conditions were 16.0057μm, 1.13%, 4.33nm respectively. Also, the results of the corrosion resistance and ion release test show that the coated sample is significantly improved compared to the substrate.

Keywords: Electrophoretic deposition (EPD), Stainless Steel 316L, PEEK, Hydroxyapatite (HA), Taguchi Design.

1. Introduction

Metals and metal alloys play a critical role in the field of biomaterials by repairing or replacing damaged load-bearing bones. Due to the increasing incidence of accidents and wars, there was a significant demand for implants. Stainless steel 316 L (medical grade) is commonly utilized as an orthopedic implant material because to its superior mechanical qualities, low cost, and ease of manufacture, in addition to its outstanding biological and chemical properties and inexpensive cost when compared to other metal implants [1], [2]. Despite these advantages, 316LSS has a number of drawbacks in terms of corrosion resistance, wear resistance, and biocompatibility. As a result, it was coating with bioceramics to enhance its biological and antibacterial capabilities [3]. One of the most important bioceramic materials is hydroxyapatite $Ca_{10}(PO_4)_6(OH)_2$, which is the major inorganic component of teeth and bone and has been widely used in biomedical applications such as implants and bone regeneration due to its high bioaffinity, bioactive, osteoconductive, and biodegradability [4][5].

As a result of the foregoing, there is a strong trend toward manipulating coating processes in order to generate optimum biomaterials with high biocompatibility, superior corrosion resistance, and high bioactivity, i.e. materials capable of tissue/bone growth and repair [4]. Thus, nonmetallic (organic or inorganic) materials such as polymers that are non-toxic, biocompatible, have a high strength, are chemically stable, and have great tribological properties will be a viable alternative for strengthening the weak spots of alloys for biological applications [5]. Chitosan is a naturally occurring cationic polysaccharide that possesses a number of significant properties including superior mechanical strength, chemical stability, biocompatibility, and antimicrobial activity [6]. These properties have enabled it to be used in biomedical implants, drug delivery, scaffolds, biosensors, and other biomedical devices [7][8].

Due to the excellent chemical and mechanical properties of polyether ether ketone (PEEK), it is considered a high-performance and bioinert material, eliciting neither a negative nor a positive response in the body. PEEK is widely used as a provisional abutments, dental implants, bone substitute in orthopedics, and clamps for removable dental prostheses [9][10][11].

Numerous research described various techniques for preparing PEEK coatings on metallic surfaces using thermal spraying [12], printing [13], and EPD from ethanolic solutions, as Wang et al. reported [14][15], Boccaccini et al. [5] and Riccardis et al.[16]. Y. Torres et al. developed a unique bio composite with exceptional infiltration by combining PEEK with bioactive glass on porous titanium substrates. We established a high degree of adhesion between the bioactive/biopolymer coatings and a high level of infiltration [17]. After annealing, Anita Sak et. al. investigated the effects of pH, time, and applied voltage on electrophoretically depositing PEEK coatings up to 70 to 90μm thick on titanium alloy (Ti–13Nb–13Zr). They discovered that the coatings were semi-crystalline, had good adhesion, and had a spherulitic morphology due to the uniform distribution of PEEK powders on the substrate [18]. On the other hand, R.B. Durairaj et al. employed the plasma spray method to deposit 5 m thick PEEK coatings on SS 316 [19].The aim of the current work is Produce a Nanobiocomposite coating layer (Polyetheretherketone (PEEK)/HA) on 316L then, optimization by using EPD AC /DC Current and to select an optimal deposit conditions have been used Taguchi method (L9) for deposition of a high-quality composite coating on a stainless steel alloy, as well as for characterizing the alloy's microstructure and significant properties, as well as for coating adherence to the alloy substrate.

2. Materials and method

Stainless steel 316L alloy has the chemical composition (0.031% C, 0.31% Si, 1.53% Mn , 0.0273% P, 0.036% S , 2.12% Mo , 16.70% Cr , 10.0% Ni, 0.0040% AL, 0.190% Co , 0.50% Cu , 68.3% Fe) .This test has been done in (State Company for Military Industries)

Both polymers were obtained from Sigma Aldrich in micrometer powder form. The polyetheretherketone (PEEK) had a mean particle size of 20 microns and the Chitosan (mid molecular weight, approximately 85 percent deacetylate, soluble in 1 percent acetic acid) was also obtained from Sigma Aldrich. The Chitosan was used as a binder for the ceramic substance. Hydroxyapatite (reagent grade, powder, synthetic) (30–100nm, 99 percent purity, white hue, 3.140 g/cm3 density) was acquired from Sigma Aldrich and employed as a coating layer. Acetic acid with purity (> 98%) and Solvents of ethanol absolute (99.9%). The electrolyte (water and ethanol). The (cathode) and (anode) was 316L stainless steel, which was cut by water jet machine with dimensions (20×15 x 5 mm) identical for EPD depositions on the substrate and distance between them at 1 cm. Samples of stainless steel were cleaned and polished. Surface grinding with emery sheets (500,800,1200 grit SIC grind) was employed to achieve the best result roughness approximately (0.02,0.03,0.06) μm respectively to enhance the bonding with substrate. The HA concentration was kept constant at 3 g/L [20], and chitosan powder (0.5 g/L) was prepared by dissolving 0.05 g in 1% acetic acid [21] and then adding it to a 100 ml beaker solution of (95 percent ethanol + 5% deionized water). This solution was used in all experiments to deposit composite films (2% peek, 4% peek and 6% peek). To ensure adequate dispersion, the suspensions were agitated for 6 hours and then ultrasonically for 30 minutes. All solutions had a pH of 4.5.

Because the primary objective of this study is to determine the near values of factors regulating the EPD, the Taguchi design of experiments was used. A careful design of factors and their levels was carried out for the deposition layer of PEEK/HA with pure chitosan. These are based on Taguchi's philosophy of experiment design L9 [22]. The factors and their associated levels for deposition of PEEK/HA layers are listed in Table 1.The deposition was carried out with 30, 60, and 90 volts at the deposition time was 1, 3 and 5 min in two stages for Power supply first DC and second AC ,were deposited on Stainless Steel alloy at room temperature. After the finishing of the EPD process remove the coated electrode out of suspension. The samples were dried in atmosphere after the completing EPD process. Optical microscopies and SEM were used to analyze the surface.

Table 1. L9 Orthogonal Array to PEEK /HA

| Sample No.	Voltage , V	Time , T	Concentration, C	Degree Of Grinding
1	1	1	1	1
2	1	2	2	2
3	1	3	3	3
4	2	1	2	3
5	2	2	3	1
6	2	3	1	2
7	3	1	3	2
8	3	2	1	3
9	3	3	2	1

3. Results and discussions

3.1. Zeta potential results

The zeta potential is a critical parameter in the EPD process because it affects both the stability of the solution and the deposition rate of coating layers with respect to their uniformity. The numbers in Table (2) indicate the zeta potential and mobility of all solutions used to deposit various layers at room temperature as shown in (fig.1 and fig.2).

Ethanol solution was used as the suspension medium for the deposition because it allows the three materials (i.e. PEEK, HA, and CHit) to be suspended correctly. The results indicated that chitosan and hydroxyapatite have positive zeta potentials; consequently, the composite particles of PEEK/HA are positively charged in the EDP suspension, and the composite particles are deposited on the cathode electrode, despite the fact that the PEEK particles are negatively charged (anion). This is because hydroxyapatite and chitosan (a natural cation polysaccharide) play a critical role in equating the suspension where the zeta potential increases as the concentration of HA is increased [23].

Table 2. The value of mobility and zeta potential

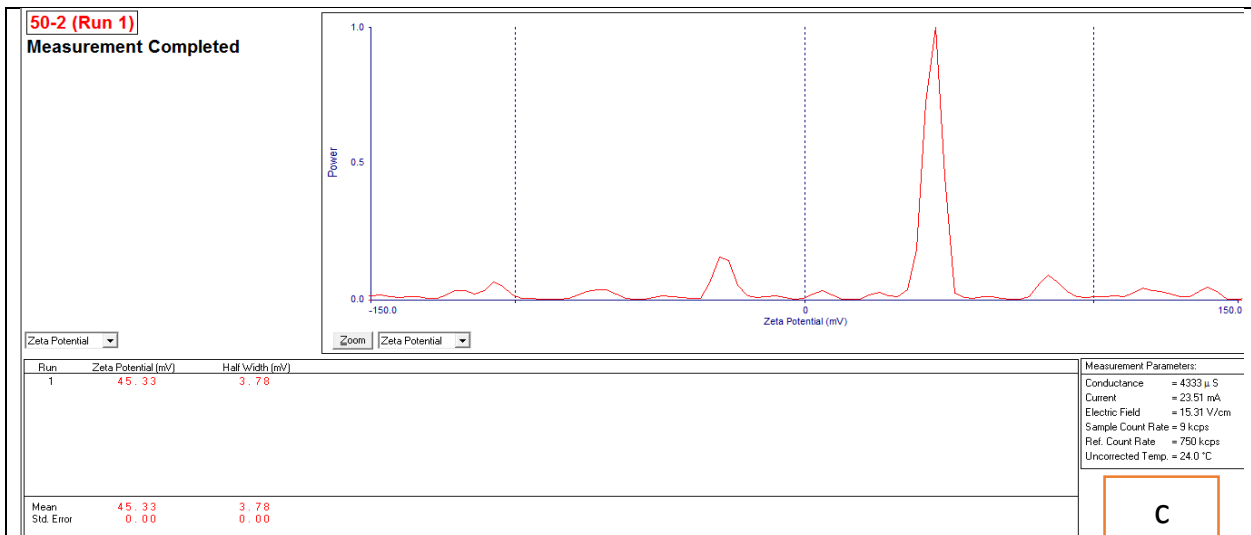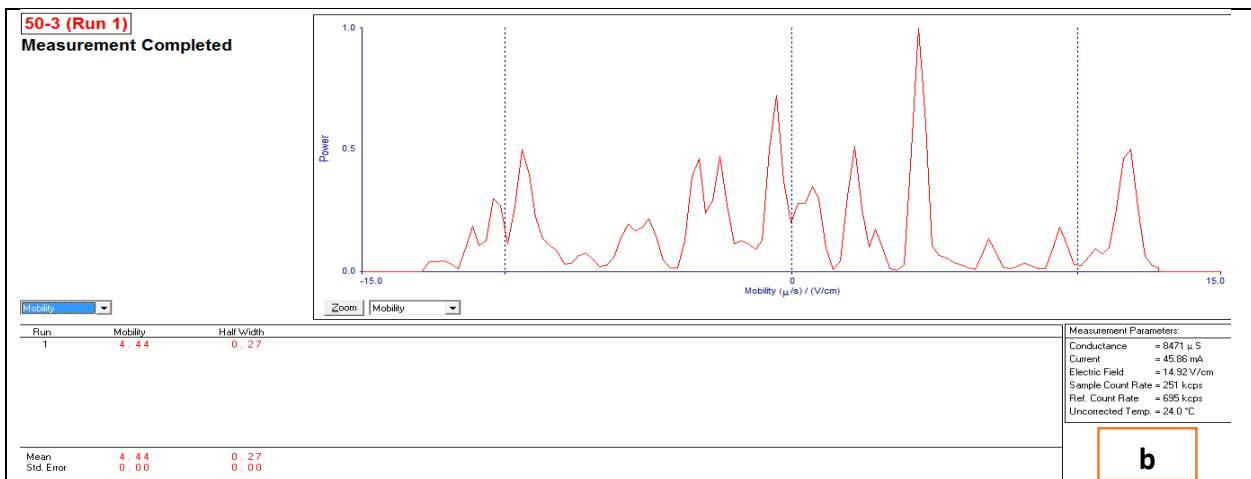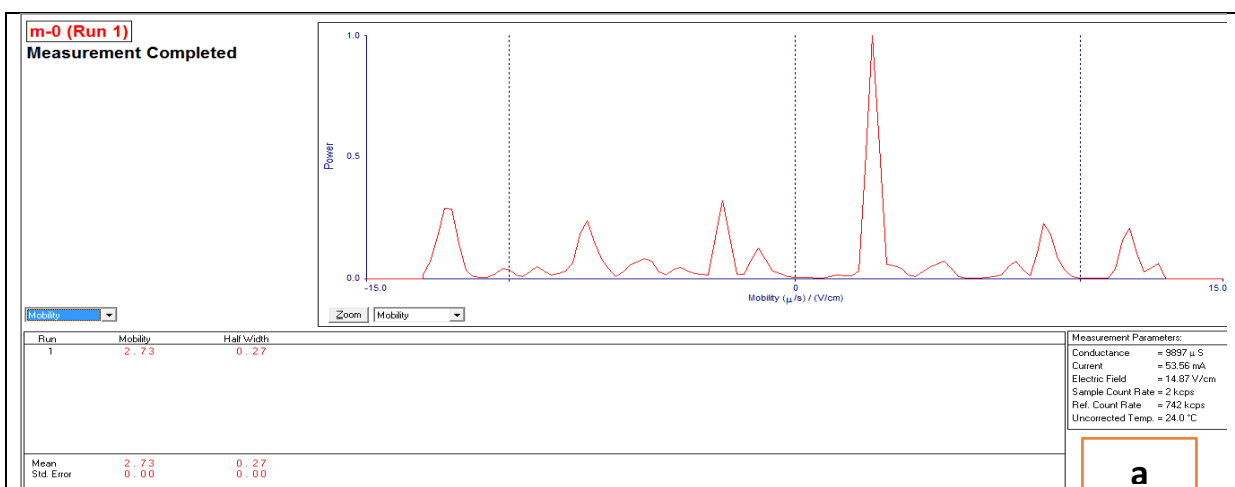| Suspension type	Zeta potential (mv)	mobility
PEEK 2%/HA	35.61	2.73
PEEK 4%/HA	57.81	4.44
PEEK 6%/HA	45.33	3.48
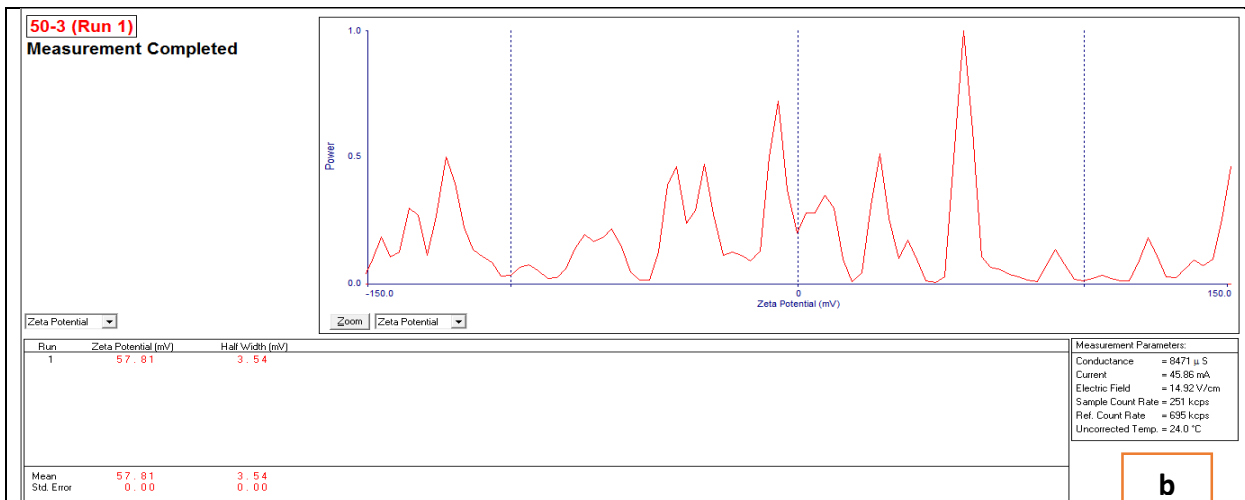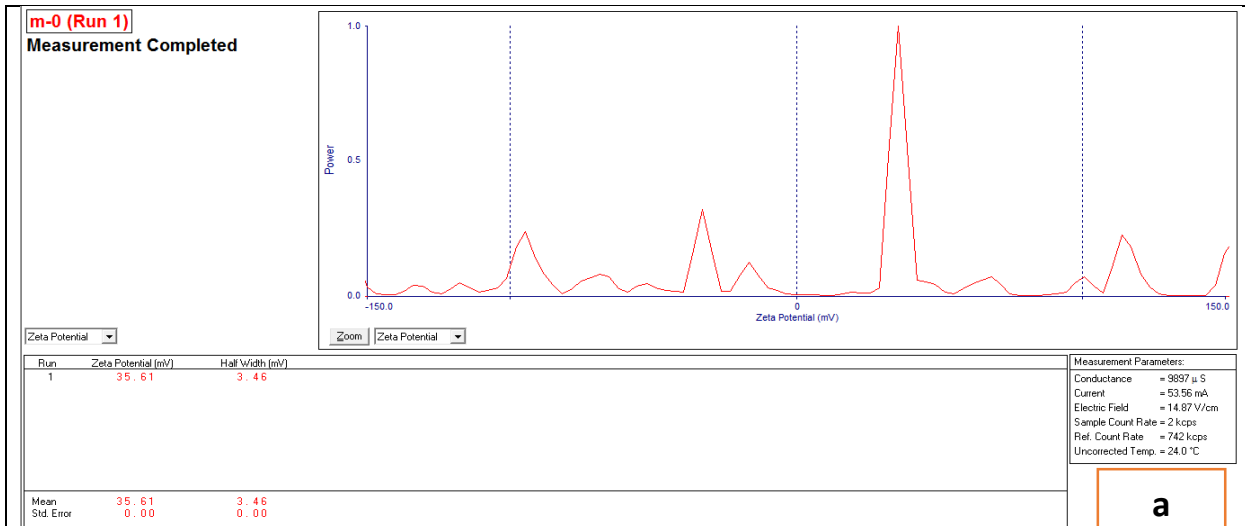
Fig. 1.   Zeta potential measurements for different solutions (a) PEEK 2% / HA (b) PEEK 4% / HA (C) PEEK 6% /HA
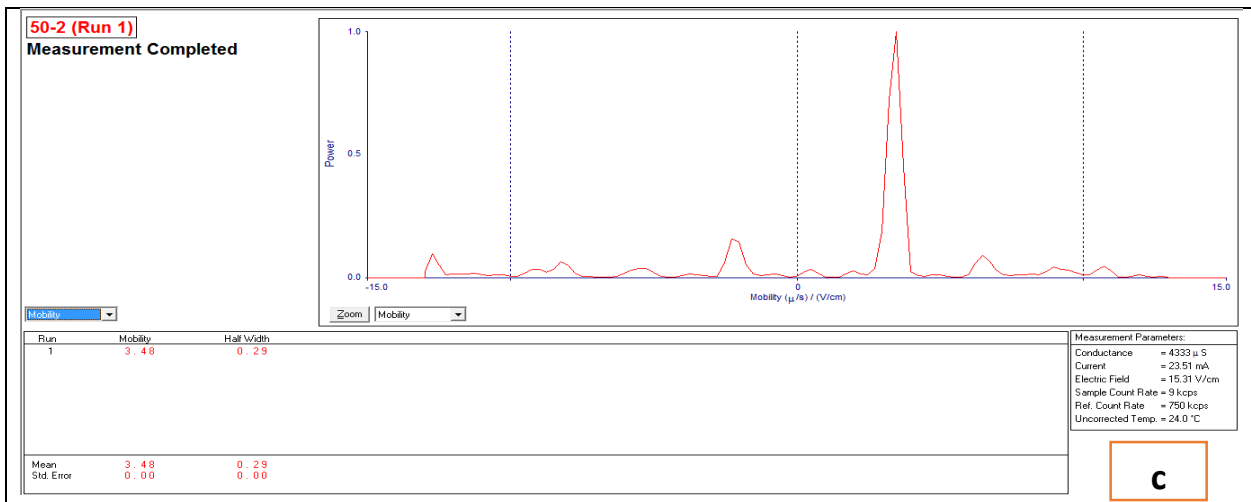
Fig. 2. Mobility measurements for different solutions (a) PEEK 2% / HA (b) PEEK 4% / HA (C) PEEK 6% /HA

3.2. cross-section result (thickness measurement)

3.2.1 For PEEK/HA coating layer by using DC

A cross-sectional image of the coating layer by light electron microscopy, was taken after the coating has dried at room temperature to check and the thickness and homogeneity of the PEEK/HA layer which was good. It was also noted that the best cross-section with the lowest porosity and the highest thickness of the PEEK/HA layer (20.1362μm) was on the surface of the substrate that has the highest roughness measure (0.06μm) at experiment (9) and lowest thickness (9.143μm) was on the surface of the substrate that has the lowest roughness value (0.02μm) at sample (3) as shown in Table 5 and Table (3 ,4)

The cross-section of nine samples of PEEK/HA coating layers utilizing DC current is shown in Figure 3. (three types roughness of substrate)

Table 3. roughness value with corresponding smoothing paper

NO.	degree of grinding paper SiC	Roughness measurement (μm)
1	500	0.06
2	800	0.03
3	1200	0.02

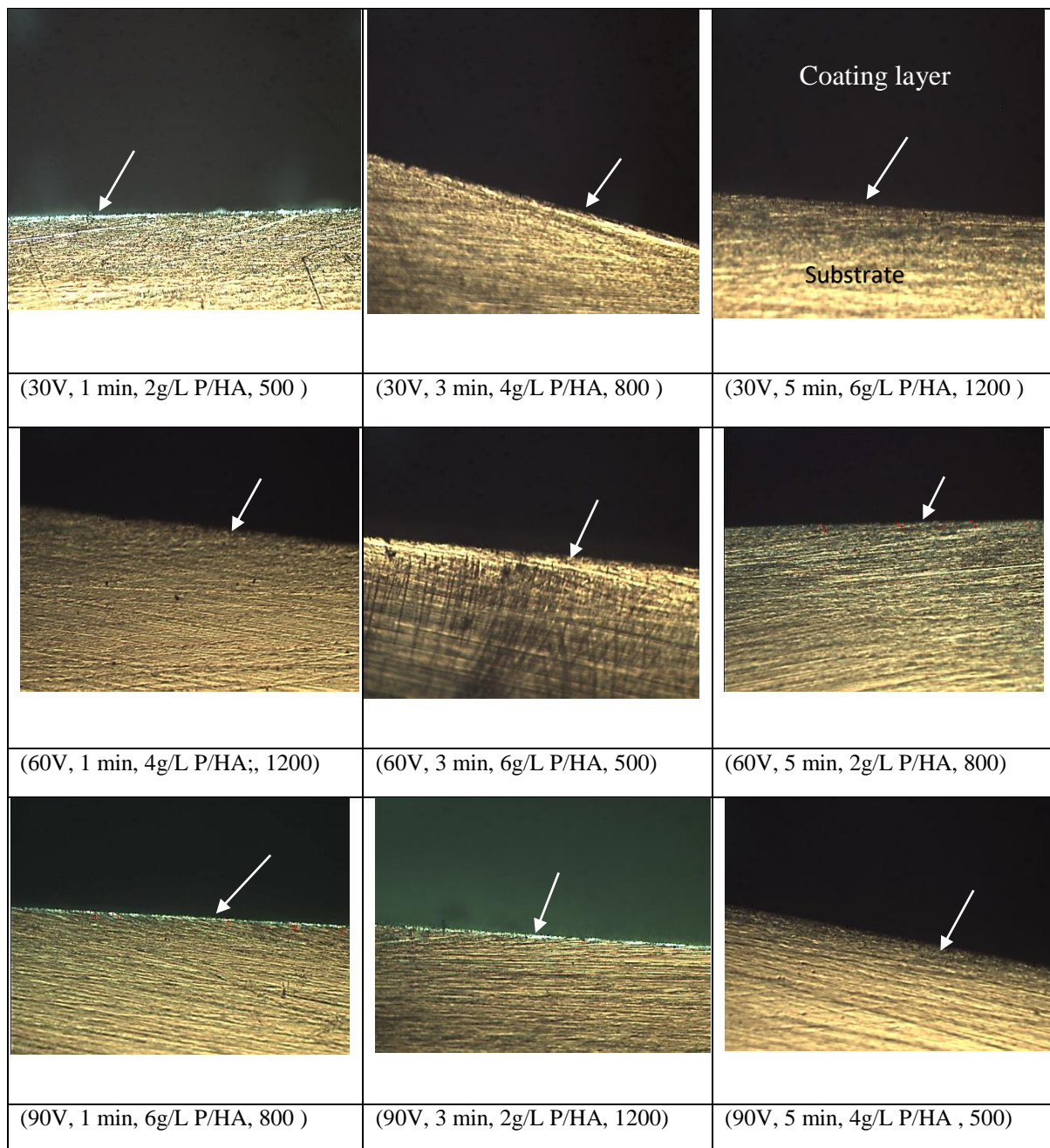|		
(30V, 1 min, 2g/L P/HA, 500)	(30V, 3 min, 4g/L P/HA, 800)	(30V, 5 min, 6g/L P/HA, 1200)
(60V, 1 min, 4g/L P/HA;, 1200)	(60V, 3 min, 6g/L P/HA, 500)	(60V, 5 min, 2g/L P/HA, 800)
(90V, 1 min, 6g/L P/HA, 800)	(90V, 3 min, 2g/L P/HA, 1200)	(90V, 5 min, 4g/L P/HA , 500)

Fig. 3. Cross sectional optical pictures of samples of (PEEK/HA) coating layers using DC

3.2.2 For PEEK/HA coating layer by using AC

Using light electron microscopy a cross-sectional image of the coating layer was acquired to verify the thickness and homogeneity of the PEEK/HA layer, which were found to be satisfactory. Additionally, as shown in Table 8, the best cross-section with the lowest porosity and the highest thickness of the PEEK/HA coating layer (16.601μm) was found on the surface of the substrate with the lowest roughness value (0.02μm) in sample (4) and the lowest thickness (11.3847μm) was found on the surface of the substrate with the highest roughness value (0.06μm) in experiment (5). (Table 3 ,4). The cross-section of nine samples of PEEK/HA coating layers utilizing AC current is shown in Fig. 4

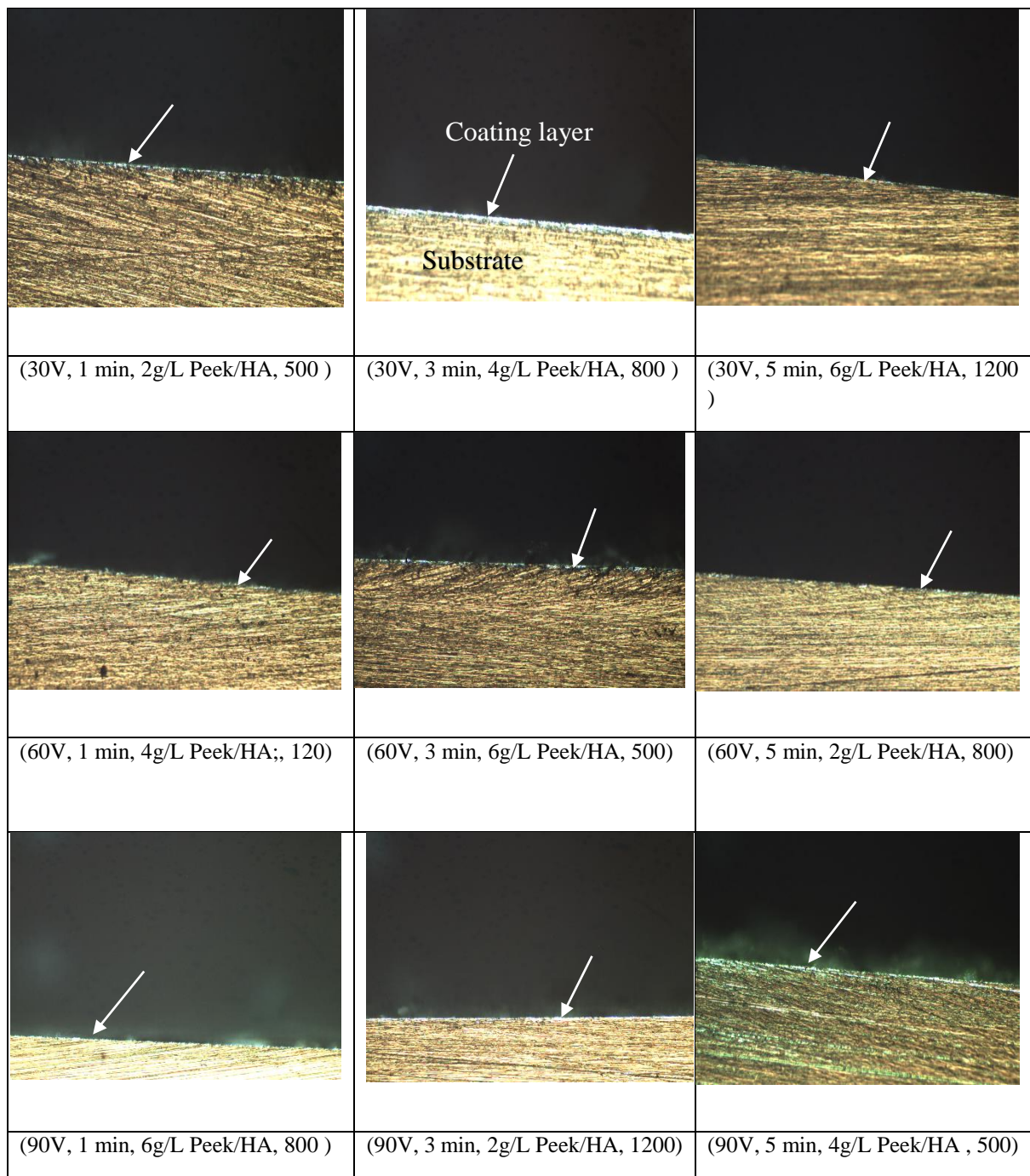| (30V, 1 min, 2g/L Peek/HA, 500)	(30V, 3 min, 4g/L Peek/HA, 800)	(30V, 5 min, 6g/L Peek/HA, 1200)
(60V, 1 min, 4g/L Peek/HA;, 120)	(60V, 3 min, 6g/L Peek/HA, 500)	(60V, 5 min, 2g/L Peek/HA, 800)
(90V, 1 min, 6g/L Peek/HA, 800)	(90V, 3 min, 2g/L Peek/HA, 1200)	(90V, 5 min, 4g/L Peek/HA , 500)

Fig. 4. Cross sectional optical pictures of samples of (PEEK/HA) coating layers using AC

3.3 Analysis of PEEK/HA layer deposition
3.3.1 Choosing the best condition via using DC

The deposition of PEEK/HA has been analyzed (table 4) using Direct Current (DC) and a range of thicknesses with a different of levels and factor values. Additionally, the SNs ratio hypothesis (greater is better) demonstrates that the experiment has a maximum SNs ratio value. The thickness of (PEEK/HA) layers was determined using Taguchi design L9 tests, as shown in Table 5. The higher thickness (20.1362μm) and S/Ns ratio (25.6612) obtained in experiment 9, were used to install the best coating layer PEEK/HA. However, based on the SNs ratio, the ideal conditions were determined to be (90 Voltage, 3 minutes, and 4% C, 0.06μm, which equated to 500 emery paper SiC), as illustrated in fig. 5. Experiments were conducted under these conditions to establish the thickness, which was determined to be (16.0057μm), which is sufficient to provide reliable PEEK/Hydroxyapatite thicknesses. The optimal conditions for solution stability were determined using zeta potential measurements; they were (57.81 mv) with a high particle mobility value (4.44).

The biggest variables affecting the deposit of the PEEK /HA layer are degree of grinding (72.60%), then concentration (15.95%), voltage (6.85%) and time (4.60) respectively, as shown in Tables (6,7).

Table 4. Taguchi approach parameters for PEEK/HA layers deposition

Experiment's	Voltage, V	Time, min	Concentrations,%	degree of grinding
1	30	1	2	0.06
2	30	3	4	0.03
3	30	5	6	0.02
4	60	1	4	0.02
5	60	3	6	0.06
6	60	5	2	0.03
7	90	1	6	0.03
8	90	3	2	0.02
9	90	5	4	0.06

Table 5. Ratio of signal to noise of Taguchi design of (L9) for PEEK/HA coating layer thickness via DC

NO.	V	T, min	C %	D	Thickness 1 μ m	Thickness 2 μ m	Thickness 3 μ m	SNRA1	MEAN1
1	30	1	2	0.06	20.1362	18.5873	12.3915	24.0255	17.0384
2	30	3	4	0.03	15.4894	12.3915	9.2936	21.2963	12.3915
3	30	5	6	0.02	10.3906	9.2936	7.7447	19.0295	9.1430
4	60	1	4	0.02	18.5873	15.4894	7.7447	21.0174	13.9405
5	60	3	6	0.06	18.6517	17.7962	12.3915	23.7867	16.2798
6	60	5	2	0.03	14.0263	10.9527	9.2936	20.7924	11.4242
7	90	1	6	0.03	12.3915	10.8426	7.7447	19.7619	10.3263
8	90	3	2	0.02	15.4894	13.9405	12.4880	22.8050	13.9726
9	90	5	4	0.06	23.2341	21.6852	15.4894	25.6612	20.1362

Table 6. Rank of thickness-controlling variables in PEEK/HA layer via using DC

Level	V	T	C%	D
1	21.45	21.60	22.54	20.95
2	21.87	22.63	22.66	20.62
3	22.74	21.83	20.86	24.49
Delta	1.29	1.03	1.80	3.87
Rank	3	4	2	1

Table 7. ANOVA for thicknesses of P/HA layer via using DC

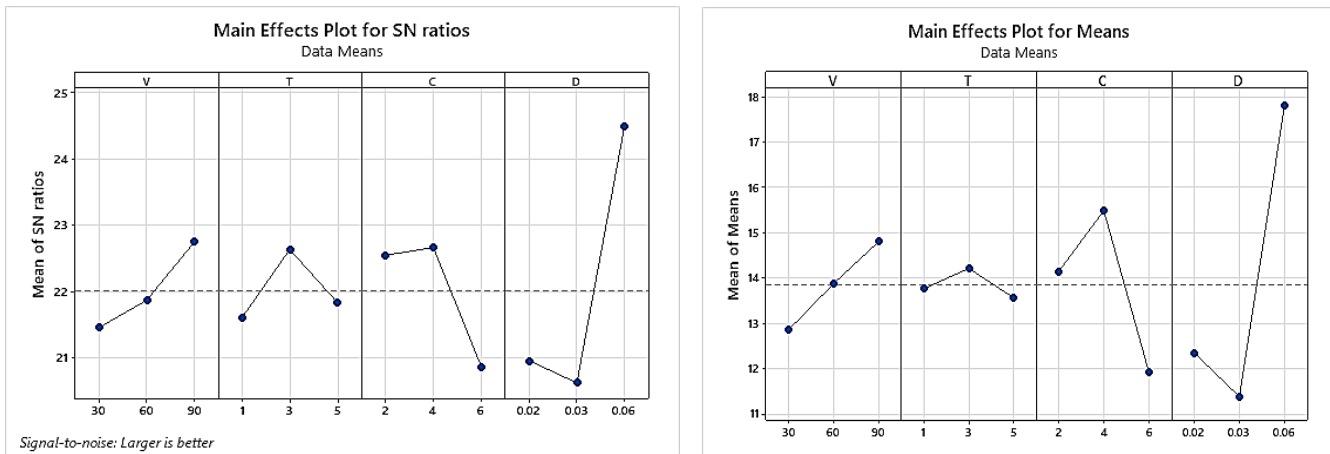| Variable	D F	Sum of squares SS	Variance MS	Contribution
V	2	2.612	1.3059	6.85
T	2	1.750	0.8750	4.60
C%	2	6.078	3.0389	15.95
D	2	27.657	13.8283	72.60
Errors	0			
Total	8	38.096		100.00

Fig. 5. Mean of reaction of SNs to PEEK/HA thickness for various factors and levels via using DC.

3.3.2 Choosing the best condition via using AC

Table 8 illustrates a variety of thicknesses formed with varied degrees of variance. Which can be used to determine the ideal circumstances for (PEEK/HA) AC coating selection. The SN (larger is best) ratio hypothesis demonstrates that the experiment with the highest SNs value implicitly has a higher quality level than the others. The thickness of the PEEK/HA layer was determined via Taguchi Design Experiments. Experiment 4 yielded the greatest thickness (16.601μm) with 60V, 1 minute, 4% C, and (0.02μm) 1200 grit sic grind However, the optimal conditions for depositing the (PEEK/HA) AC layer are (60V, 5 minutes, 4% C, and 0.03μm, which corresponds to 800 emery paper SiC), as illustrated in Figure 6. To test the circumstances, experiments were conducted under these conditions and it was determined that the thickness is (12.9731μm), which is sufficient to get a reliable PEEK/Hydroxyapatite thicknesses. According to the Taguchi Design (L9) Signal to Noise Ratio for (PEEK/HA) AC Coating thickness, the most significant elements impacting this process are voltage (13.79%), time (10.42%), then concentration (45.84%), followed by degree of grinding (29.95%) as shown in (Tables 9,10).

Table 8. Ratio of signal to noise of Taguchi design of (L9) for PEEK/HA coating layer thickness via AC

NO.	V	T, min	C %	D	Thickness 1 μ m	Thickness 2 μ m	Thickness 3 μ m	SNRA1	MEAN1
1	30	1	2	0.06	17.1086	10.9527	6.1958	18.9960	11.4190
2	30	3	4	0.03	17.1086	15.5667	12.3915	23.2927	15.0223
3	30	5	6	0.02	14.2805	12.3915	9.2936	21.1551	11.9886
4	60	1	4	0.02	20.3731	15.4894	13.9405	24.0808	16.6010
5	60	3	6	0.06	15.5667	10.8426	7.7447	20.1018	11.3847
6	60	5	2	0.03	17.0384	15.5667	14.0263	23.7488	15.5438
7	90	1	6	0.03	15.4894	12.4880	9.7964	21.5489	12.5912
8	90	3	2	0.02	13.9405	11.2765	9.2936	20.8640	11.5035
9	90	5	4	0.06	18.8437	15.7962	10.8426	22.9158	15.1608

Table 9. Rank of thickness-controlling variables in PEEK/HA layer via using AC

Level	V	T	C%	D
1	21.15	21.54	21.20	22.03
2	22.64	21.42	23.43	22.86
3	21.78	22.61	20.94	20.67
Delta	1.50	1.19	2.49	2.19
Rank	3	4	1	2

Table 10. ANOVA for thicknesses of PEEK/HA layer via using AC

Variable	D F	Sum of squares SS	Variance MS	Contribution
V	2	3.385	1.693	13.79

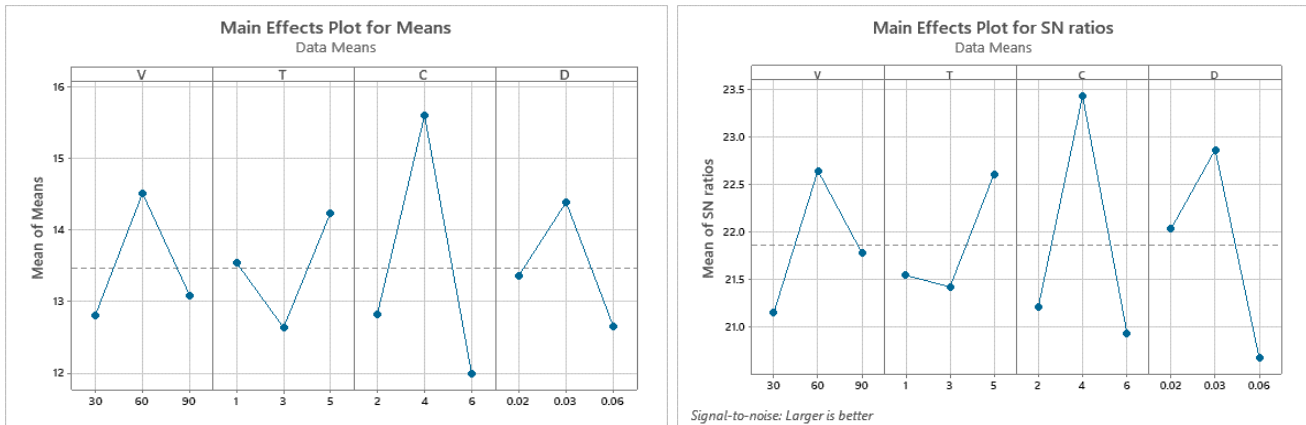| T	2	2.558	1.279	10.42
C%	2	11.253	5.626	45.84
D	2	7.351	3.675	29.95
Errors	0			
Total	8	24.546		100.00

Fig. 6. Mean of reaction of SNs to PEEK/HA thickness for various factors and levels via using AC

3.3.3 Selection of finale optimum conditions for PEEK/HA layer Based on adhesion

Due to adhesion is the key output characteristic in this work, it was determined using the ASTM D3359-B standard to determine the best current (Dc or Ac) that would provide the best adhesion to the deposited coating by the EPD technique of finale optimum circumstances for depositing (PEEK/HA) layer. The adhesive tape test method was used to determine the adhesion strengths of coatings on stainless steel 316L substrates in order to evaluate the qualitative bonding of coating. The percentage of coating layer area removed was determined using a scale of 2mm.

The DC sample had better adhesion with a removal area of (9%), compared to (11%) for the AC sample, as shown in Figure 7. With this result, we will conduct the rest of the tests on the DC sample to evaluate its coating layer for use in medical applications.
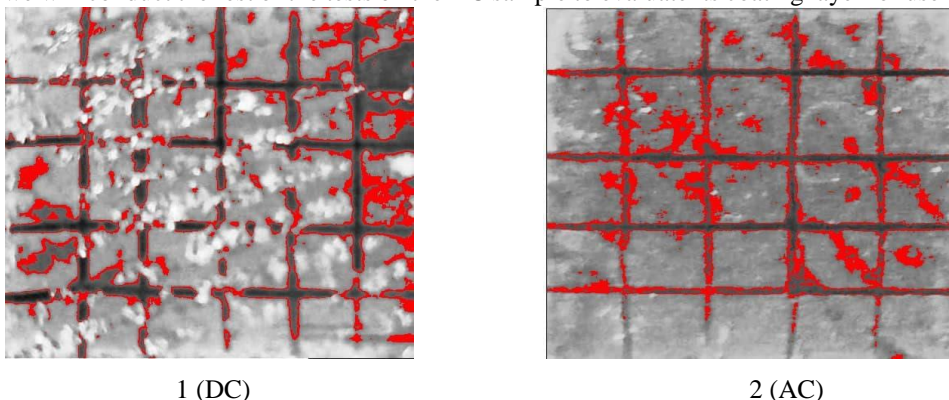

1 (DC)   2 (AC)

Fig. 7. Optical images for deposited coatings of PEEK/HA (1) Removal Area ratio of coating layer 9% . (2) Removal Area ratio of coating layer 11%.

3.4 Metallurgical test result for (PEEK/HA) DC layer

Optical microstructure and SEM employed to calculate thickness and study the microstructure of coating layers.

It is possible to observe homogeneous coating layers and uniformity under an optical microscope under optimal conditions. They also contain a low percentage of porosities and have an adequate thickness when the layers are observed under an optical microscope. The thickness of PEEK/HA coating layer was (16.005 μm) [3]. As the high thickness of the coating layers has good properties because it the increase of it lead to improvement of corrosion resistance and reduce Cr ion release. Optical images for topography and cross section for the samples coating are shown in Fig.8. For confirmation purpose from the results of optical microstructure observations. Scanning electron microscopy (SEM) was used to identify the surfaces topography of samples the coatings. SEM and optical microscope images (Fig. 9, 8) show that interface clearly gives an evidence of uniform of coatings layers without cracks as expected. It should be noted that it may seems that there are cracks on the surface of the coating as shown Fig. 11, but in fact it is the end of a layer of coating accumulated on top of each other (overlap).
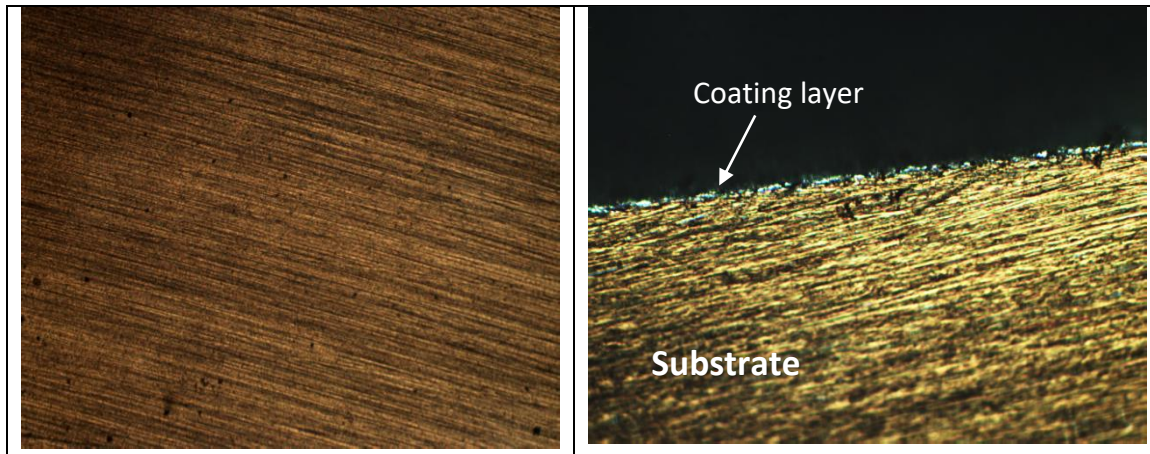
Fig. 8. Optical images of topography and cross section for one layer PEEK/HA
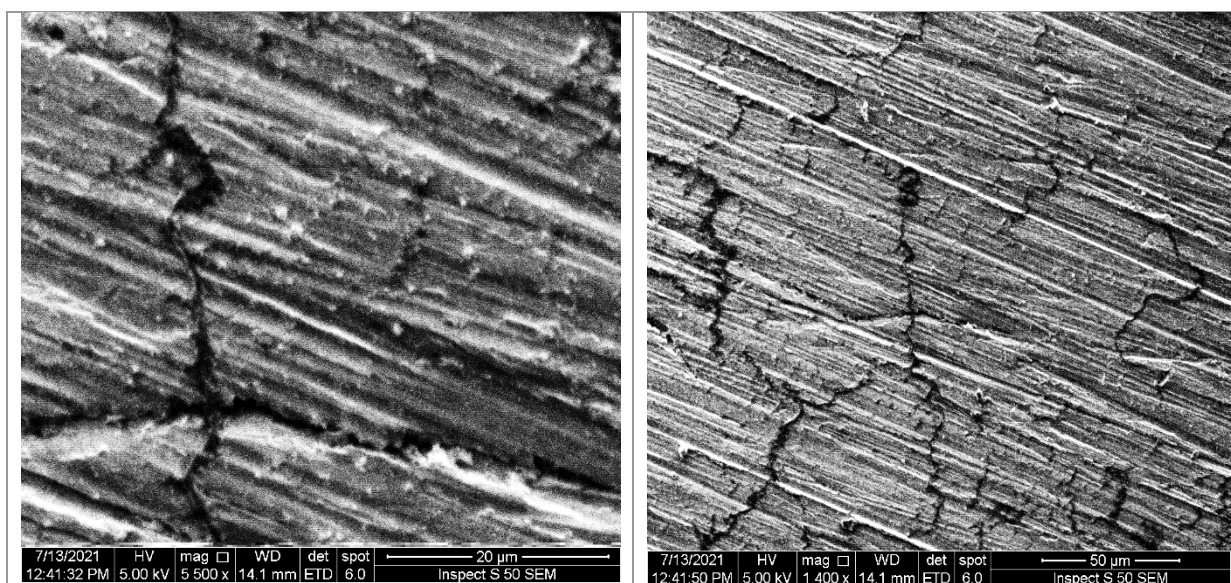

Fig. 9. SEM images of topography for one layer PEEK/HA

The level of porosity in surface optical pictures is determined using the Image J program for a sample PEEK/HA layer are (1.13 %).The red color presented the porosities can be seen in the fig.10.The suspension properties effect amount of porosity contain (concentration, zeta potential of particles and particles distribution). And as a higher zeta potential represents better dispersion.As a result, the movement and distribution of the coating solution particles is better , it can be seen that the pH value for EPD should be at pH less than 7.0. We note that the value of the value of PH for the (PEEK/ HA) is 4 within average and good and also, zeta potential value is (57.81mv) and the particle mobility value is (4.44) in the (PEEK/HA) solution .This helps to obtain a layer of paint with a pore ratio within the required rate because the fact that pores are required for tissue development, allow penetration of bone tissue, this give best bio integration and good mechanical stability for implant in body and the porous surface enhances mechanical interaction between the implant biomaterial and the native tissue that surrounds it [24] . In contrast, increasing the porosity has a negative impact on the mechanical properties of the material. Open porosity has a direct effect on the ability of wanted and undesirable fluids, cells, or germs to enter, and as such should be maintained at an acceptable average.
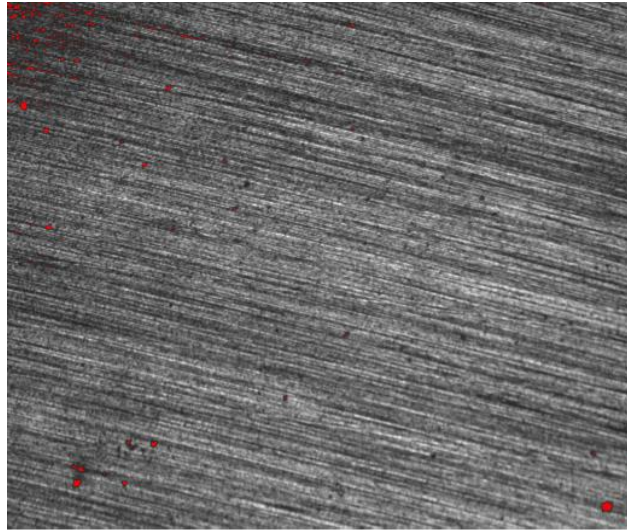
Fig. 10. Porosities estimation for one layer PEEK/HA

The roughness of the substrate is crucial in the EPD process for bone replacement applications in particular. Coating layer roughness has an effect on (adhesion, differentiation and proliferation) to implants, resulting in a strong connection between the implant and human host bone. Nano roughness measured used AFM technique for PEEK/HA coating layer and the value of Ra was (4.33nm) . Fig.11. illustrates the topography of density particles for covering PEEK/HA layer. The average diameter particles of PEEK/HA coating layer are (38.97nm).
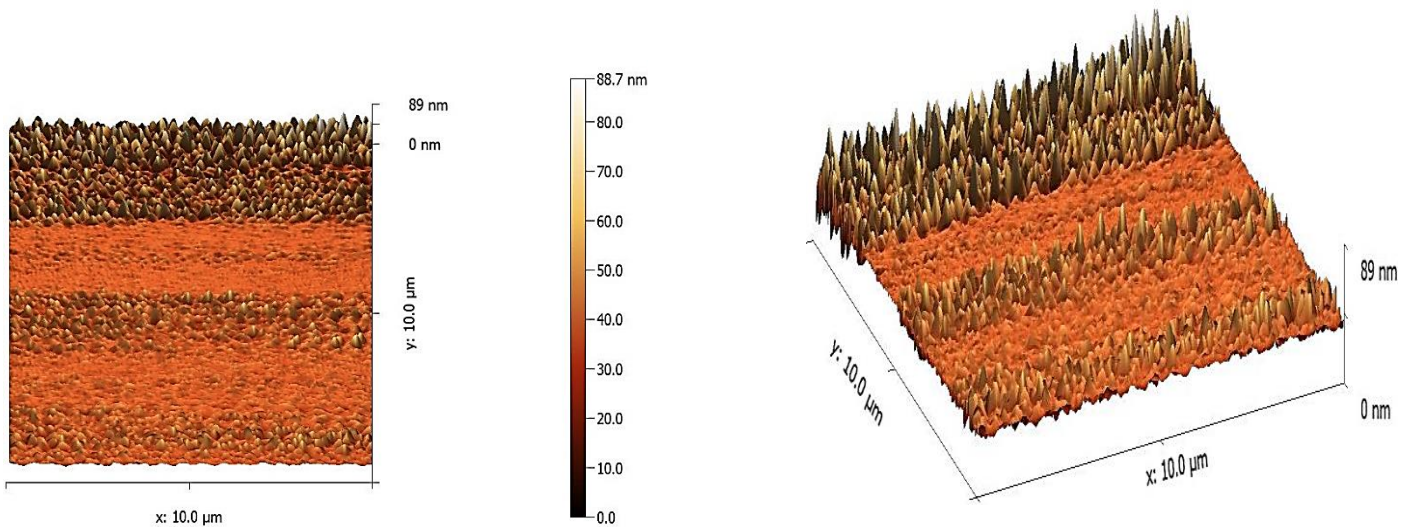

Fig. 11. The two- and three-dimensional (2D,3D) features of (AFM) images for PEEK/HA layer

3.5. Structural results

Before and after EPD coating with PEEK/HA layer, XRD analysis was utilized to identify the phases in AISI 316 L alloy.

The stainless steel phase spectrum demonstrates the existence of austenite phase (γ) with three different 2θ peaks at [74.76° (220), 43.76° (111), 50.84° (200)] referred by symbol ($\star$) as shown in figure 12. PEEK+ chitosan +HA coating layer which obtained by EPD method at a constant potential of 90 V as shows in Fig. 13. mixture phases of strongest peaks for PEEK (43.4816°, 21.8578° and 39.6625°) referred by symbol ($\bullet$) and phases of Hydroxyapatite [(43.4816° (113), 31.7813° (113) and 32.7916° (300))] referred by symbol ($\blacktriangle$) and additionally another phases of substrate SS 316L (74.5344° ,43.4861 ° and 50.6354°) . The highest intensity for PEEK/HA was found at 2θ of 43.4816°.

All peaks in the XRD pattern of Stainless Steel and HA are identical to those in JCPDS card No 33-0397 and 09-0432, respectively, confirming the purity of the Hydroxyapatite and substrate. The results clearly demonstrate the presence of major peaks for stainless steel, hydroxyapatite, and polyether etherketon with little line broadening, indicating a well-crystallized composite coating. Furthermore, the patterns exhibit no structural changes in crystallinity or stoichiometry, confirming the durable character of the PEEK/HA coatings created without the need of thermal treatment, as is often required [25], which may be attributed to the use of chitosan biopolymer as a binder [26].

Furthermore, the XRD pattern of composites in Fig. 13 clearly shows that no additional peaks have developed, indicating that interfacial bonding has occurred between the component of coating particles.
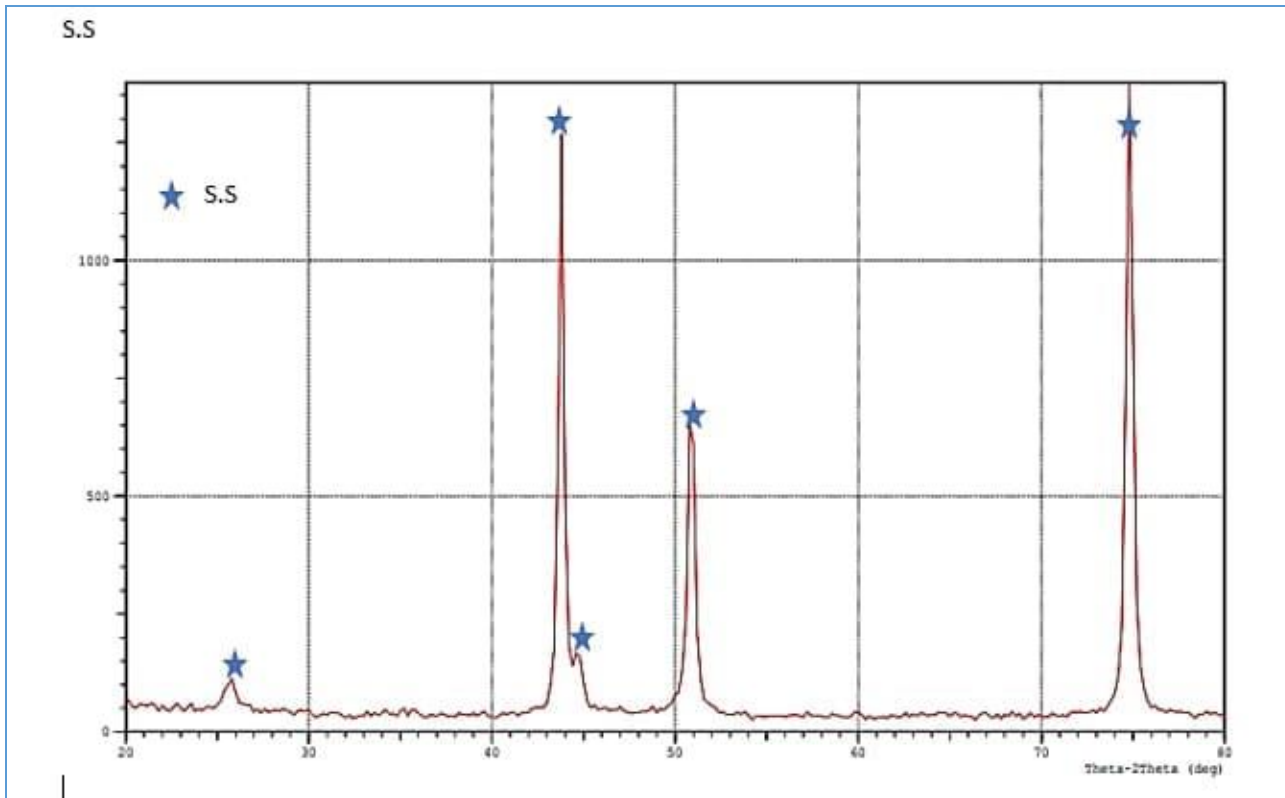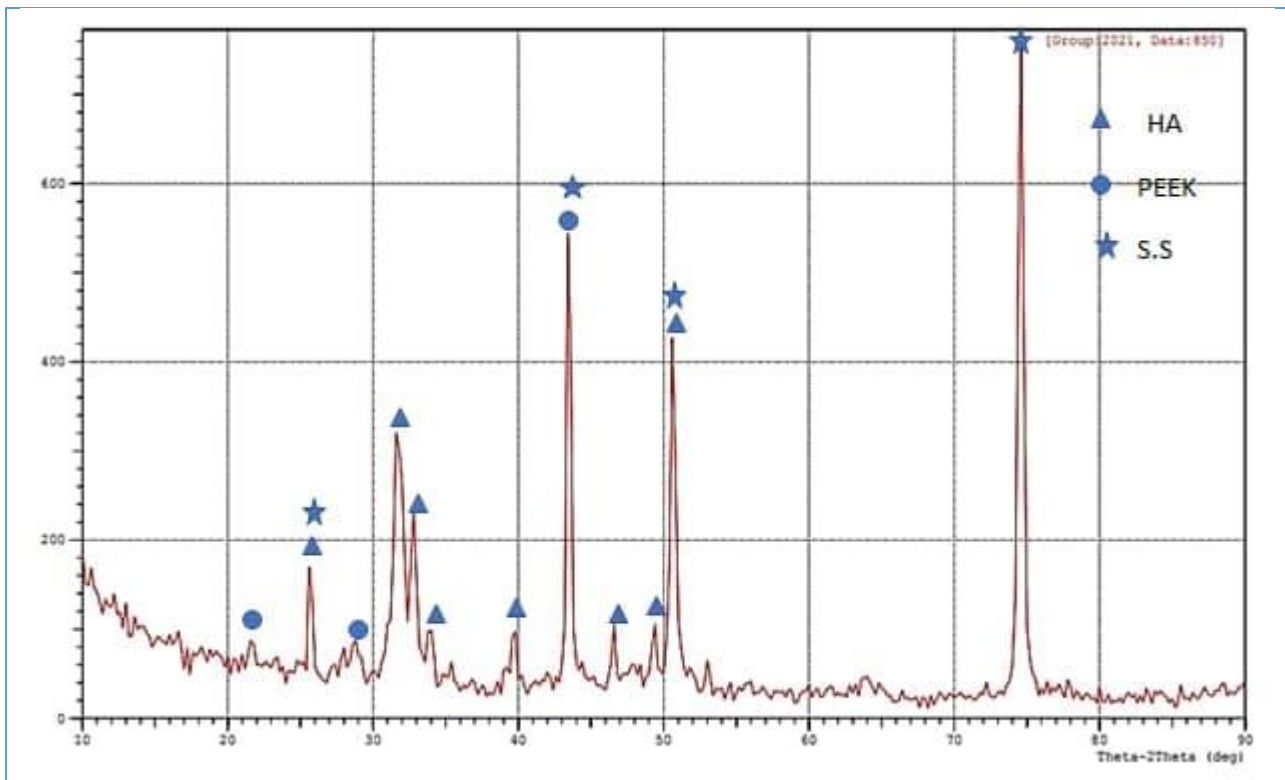

Fig. 12. XRD pattern of Stainless Steel 316L alloy.

Fig. 13. XRD is the pattern of PEEK/HA layer

3.6 Chemical test result for (PEEK/HA) DC layer
3.6.1 Corrosion Behavior of the Coating

Polarization curves for SS 316L with and without coating in SBF' solution at 37 °C, Stainless Steel 316L without coated, PEEK/HA coating layer shown in figure 16.

Low current density indicates a high corrosion resistance in the coated stainless steel alloy. In compared to SS 316L alloy, the coated–Stainless Steel alloy exhibits an increase in corrosion resistance, as characterized by low anodic current densities. This is due to the stability of the solution, the uniformity and homogeneity of the coating layer and the absence of cracks. Applying electrochemical corrosion assessment in the biological fluids of developed PEEK/HA coating layer. At a temperature of 37 °C, it was demonstrated that coated specimens of SS 316L alloy exhibit excellent corrosion resistance in the SBF solution. Table 11. contain of parameters corrosion characteristics derived from cyclic curves. The corrosion of coated samples with PEEK/HA layer coating is significantly reduced, but the potential is increased. The values of the passivation voltages (Epp) and (Ipp), as well as the current, for SS 316L uncoated, one Layer PEEK/HA as shown in the figure 14. Both values of the result are shown in Table 11.

Table 11. Results of electrochemical corrosion parameters following corrosion testing on all Layers upon immersion in SBF.

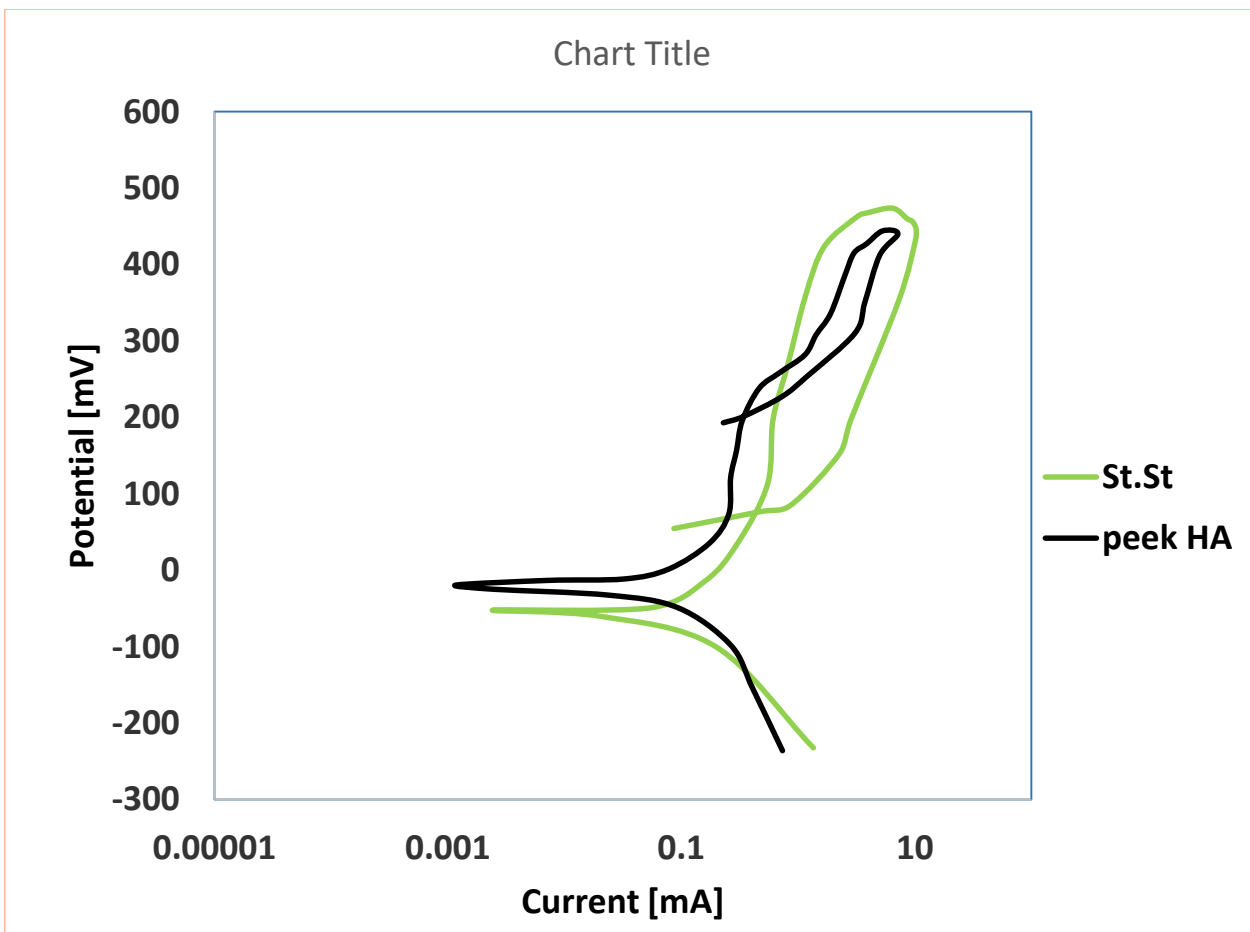| NO.	Type of sample	E pit	I pit
1	Substrate	0.468	76.67
2	One layer PEEK/HA	0.338	201

Fig. 14. Cyclic polarization curves of (1) substrate (2) one layer PEEK/HA

3.6.2 Cr Ion Release Measurements

Metal release increased , results in the secretion of proinflammatory cytokines. Additionally, if sufficient amounts of chromium ions are liberated from AISI Stainless Steel 316L alloys, they may trigger (elicit) allergic dermatitis (eczema) [27].Chromium ion release test is used to insure the capability of SS 316L alloys to use in human body. The amount of released chromium per sample surface in ppb (par pier billion) was converted to ppm (par pier million). Table 12 show that the released Cr ion content of the samples from Substrate, One layer PEEK/HA for the immersion at four week (0.0073,0.00162, respectively) in 0.9% NaCl solution. Where we note that the increases the release of chromium ions greater for substrate, but in coating sample there is release of Cr ions, but less compered with substrate and is considered safe within the human body. This is due to the stability of the solution, the uniformity and homogeneity of the coating layer and the absence of cracks. Shown Fig. 15. Cr ion released in 0.9% NaCl for samples at four week .

That the amount of Cr ion release proportion with the porosity because the exposed samples surface to 0.9% NaCl with high porosity or the low porosity It has a certain effect, especially with the difference in the coating and its granular size and with

increasing of thickness. Cr ion release into immersion solution is eliminated by these coatings, which form a physical and chemical barrier against Cr oxidation and affect the oxidation routes of Cr [28].
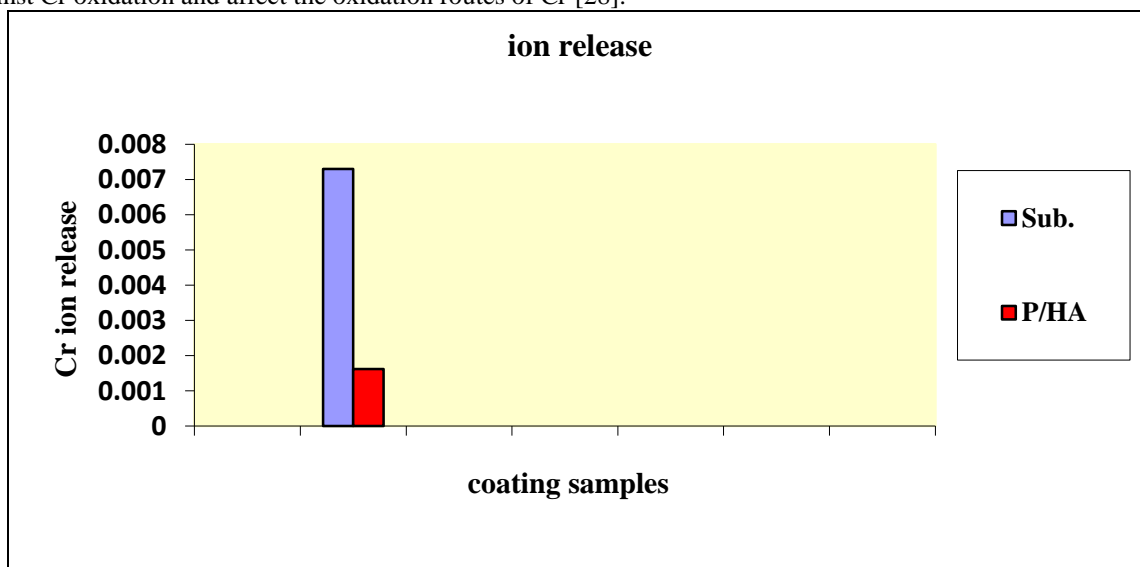

Fig. 15. Cr ion released in 0.9% NaCl for samples at four week

Table 12. Cr ion release of coating samples.

NO.	Type of sample	Cr Ion Release Four week (ppm)
1	Substrate	0.0073
3	One layer PEEK/HA	0.00162

4. Conclusion

The major conclusions observe for the present work are as follows :-
1- According to the findings of the evaluation, the optimal conditions for depositing the PEEK/HA layer were 90 V, 3 minutes, 4 g/L, and 500 degree grinding with DC current.
2- According to the findings of the evaluation, the optimal conditions for depositing the PEEK/HA layer were 60 V, 5 minutes, 4 g/L, and 800 degree grinding with AC current.
3- The optimum conditions for deposit PEEK/HA DC layer had better adhesion with a removal area of (9%), compared to (11%) for the optimum conditions AC coating layer. With this result and based on the adhesion, we will conduct the rest of the tests on the DC sample to evaluate its coating layer for use in medical applications
4- XRD analysis proved that EPD technique didn't affect phases and compositions of materials used in coating according to XRD pattern Because the work was done at room temperature using chitosan and the sintering process was not used.
5- The polarization curves are shown good corrosion resistance for coated sample and Cr ion released from coated SS 316L in 0.9% NaCl is decreased   compared with substrate of SS 316L 0.0073 ppm to 0.00162 ppm for (PEEK/HA) layer that is, with an improvement in the direction of decreasing the release of ions, about 80%.

References

[1]   V. Azar, B. Hashemi, and M. R. Yazdi, "The effect of shot peening on fatigue and corrosion behavior of 316L stainless steel in Ringer's solution," *Surf. Coatings Technol.*, vol. 204, no. 21–22, pp. 3546–3551, 2010.
[2]   D. Gopi, S. Ramya, D. Rajeswari, and L. Kavitha, "Corrosion protection performance of porous strontium hydroxyapatite coating on polypyrrole coated 316L stainless steel," *Colloids Surfaces B Biointerfaces*, vol. 107, pp. 130–136, 2013.
[3]   M. H. Abdulkareem, A. H. Abdalsalam, and A. J. Bohan, "Influence of chitosan on the antibacterial activity of composite coating (PEEK/HAp) fabricated by electrophoretic deposition," *Prog. Org. Coatings*, vol. 130, pp. 251–259, 2019.
[4]   Q. Chen, Y. Liu, Q. Q. Yao, K. Zheng, M. Pischetsrieder, and A. R. Boccaccini, "Multilayered bioactive composite coatings with drug delivery capability by electrophoretic deposition combined with layer-by-layer deposition," *Adv. Biomater. Devices Med.*, vol. 1, no. 1, 2014.
[5]   A. R. Boccaccini, C. Peters, J. A. Roether, D. Eifler, S. K. Misra, and E. J. Minay, "Electrophoretic deposition of polyetheretherketone (PEEK) and PEEK/Bioglass® coatings on NiTi shape memory alloy wires," *J. Mater. Sci.*, vol. 41, no. 24, pp. 8152–8159, 2006.
[6]   M. A. Akhtar, C. E. Mariotti, B. Conti, and A. R. Boccaccini, "Electrophoretic deposition of ferulic acid loaded bioactive glass/chitosan as antibacterial and bioactive composite coatings," *Surf. Coatings Technol.*, vol. 405, p. 126657, 2021.
[7]   D. Zhitomirsky, J. A. Roether, A. R. Boccaccini, and I. Zhitomirsky, "Electrophoretic deposition of bioactive glass/polymer

composite coatings with and without HA nanoparticle inclusions for biomedical applications," *J. Mater. Process. Technol.*, vol. 209, no. 4, pp. 1853–1860, 2009.

[8]   M. Ishihara, H. Hattori, and S. Nakamura, "A review on biomedical applications of chitosan-based biomaterials," *Int. J. Pharm. Biol. Sci*, vol. 6, pp. 162–178, 2015.

[9]   X. Han *et al.*, "Carbon fiber reinforced PEEK composites based on 3D-printing technology for orthopedic and dental applications," *J. Clin. Med.*, vol. 8, no. 2, p. 240, 2019.

[10]   S. M. Kurtz, *PEEK biomaterials handbook*. William Andrew, 2019.

[11]   D. Almasi, N. Iqbal, M. Sadeghi, I. Sudin, M. R. Abdul Kadir, and T. Kamarul, "Preparation methods for improving PEEK's bioactivity for orthopedic and dental application: a review," *Int. J. Biomater.*, vol. 2016, 2016.

[12]   G. Zhang, H. Liao, M. Cherigui, J. P. Davim, and C. Coddet, "Effect of crystalline structure on the hardness and interfacial adherence of flame sprayed poly (ether–ether–ketone) coatings," *Eur. Polym. J.*, vol. 43, no. 3, pp. 1077–1082, 2007.

[13]   G. Zhang, H. Liao, H. Li, C. Mateus, J.-M. Bordes, and C. Coddet, "On dry sliding friction and wear behaviour of PEEK and PEEK/SiC-composite coatings," *Wear*, vol. 260, no. 6, pp. 594–600, 2006.

[14]   C. Wang, J. Ma, and W. Cheng, "Formation of polyetheretherketone polymer coating by electrophoretic deposition method," *Surf. Coatings Technol.*, vol. 173, no. 2–3, pp. 271–275, 2003.

[15]   J. Ma, C. Wang, and C. H. Liang, "Colloidal and electrophoretic behavior of polymer particulates in suspension," *Mater. Sci. Eng. C*, vol. 27, no. 4, pp. 886–889, 2007.

[16]   I. Corni, N. Neumann, D. Eifler, and A. R. Boccaccini, "Polyetheretherketone (PEEK) coatings on stainless steel by electrophoretic deposition," *Adv. Eng. Mater.*, vol. 10, no. 6, pp. 559–564, 2008.

[17]   Y. Torres *et al.*, "Electrophoretic deposition of PEEK/45S5 bioactive glass coating on porous titanium substrate: influence of processing conditions and porosity parameters," in *Key Engineering Materials*, 2016, vol. 704, pp. 343–350.

[18]   A. Sak *et al.*, "Influence of polyetheretherketone coatings on the Ti–13Nb–13Zr titanium alloy's bio-tribological properties and corrosion resistance," *Mater. Sci. Eng. C*, vol. 63, pp. 52–61, 2016.

[19]   R. B. Durairaj, S. Ramachandran, B. Sathish Kumar, and T. Sekhar Vijay, "Characterization of Hydroxyapatite Coated SS316L for Biomedical Application," in *Applied Mechanics and Materials*, 2015, vol. 813, pp. 140–144.

[20]   Makarim Hazim Abdulkareem, "Optimizing of Electrophoretic Deposition Parameters and Characterization of Nanobiocomposites Functionally Graded Hydroxyapatite-Yttria Partially Stabilized Zirconia," University of Technology, 2017.

[21]   S. Mahmoodi, L. Sorkhi, M. Farrokhi-Rad, and T. Shahrabi, "Electrophoretic deposition of hydroxyapatite–chitosan nanocomposite coatings in different alcohols," *Surf. Coatings Technol.*, vol. 216, pp. 106–114, 2013.

[22]   R. R. Rawdan, M. H. Abdulkareem, and A. Mustafa, "Optimizing of Coating Layers Parameters of (Nano Hydroxyapatite/TiO2 NPs) on Nitinol SMAs by Electrophoretic Deposition," *Eng. Technol. J.*, vol. 38, no. 4, pp. 530–544, 2020.

[23]   F. E. Baştan, M. A. U. Rehman, Y. Y. Avcu, E. Avcu, F. Üstel, and A. R. Boccaccini, "Electrophoretic co-deposition of PEEK-hydroxyapatite composite coatings for biomedical applications," *Colloids Surfaces B Biointerfaces*, vol. 169, pp. 176–182, 2018.

[24]   M. J. Sultana and F. R. S. Ahmed, "Porous biomaterials: classification, fabrication and its applications in advanced medical science," *Am. J. Nanosci.*, vol. 4, no. 2, pp. 16–20, 2018.

[25]   T. M. Sridhar, U. K. Mudali, and M. Subbaiyan, "Preparation and characterisation of electrophoretically deposited hydroxyapatite coatings on type 316L stainless steel," *Corros. Sci.*, vol. 45, no. 2, pp. 237–252, 2003.

[26]   M. J. Kadhim, N. E. Abdullatef, and M. H. Abdulkareem, "Optimization of Nano Hydroxyapatite/chitosan Electrophoretic Deposition on 316L Stainless Steel Using Taguchi Design of Experiments," *Al-Nahrain J. Eng. Sci.*, vol. 20, no. 5, pp. 1215–1227, 2017.

[27]   D. Bregnbak, J. D. Johansen, M. S. Jellesen, C. Zachariae, T. Menné, and J. P. Thyssen, "Chromium allergy and dermatitis: prevalence and main findings," *Contact Dermatitis*, vol. 73, no. 5, pp. 261–280, 2015.

[28]   C. T. Kwok, P. K. Wong, F. T. Cheng, and H. C. Man, "Characterization and corrosion behavior of hydroxyapatite coatings on Ti6Al4V fabricated by electrophoretic deposition," *Appl. Surf. Sci.*, vol. 255, no. 13–14, pp. 6736–6744, 2009.